LEAF PHENOLOGY FROM CANOPY TO LANDSCAPE: A MULTI-SCALE ANALYSIS IN SEASONALLY DRY TROPICAL FORESTS

Andeise Cerqueira Dutra[1], Desiree Ramos[2], Leonor Patricia Morellato[3], Magna Moura[4], Egidio Arai[5], Alfredo Huete[6], Yosio Edemir Shimabukuro[7], Bruna Alberton[8]

[1]Graduate Program in Remote Sensing - PGSER, Earth Observation and Geoinformatics Division - DIOTG, National Institute for Space Research - INPE, São José dos Campos, Brazil, andeise.dutra@inpe.br; [2]Department of Botany, Institute of Biosciences, São Paulo State University, Rio Claro, Brazil, dm.ramos@unesp.br; [3]Department of Botany, Institute of Biosciences, São Paulo State University, Rio Claro, Brazil, patricia.morellato@unesp.br; [4]Brazilian Agricultural Research Corporation, Embrapa Semiárido, Petrolina, Pernambuco, Brazil, magna.moura@embrapa.br; [5]Earth Observation and Geoinformatics Division - DIOTG, National Institute for Space Research - INPE, São José dos Campos, Brazil, egidio.arai@inpe.br; [6]School of Life Sciences, University of Technology Sydney, Sydney, Australia, alfredo.huete@uts.edu.au; [7]Earth Observation and Geoinformatics Division - DIOTG, National Institute for Space Research - INPE, São José dos Campos, Brazil, yosio.shimabukuro@inpe.br; [8]Department of Botany, Institute of Biosciences, São Paulo State University, Rio Claro, Brazil, bruna.alberton@unesp.br;

ABSTRACT

Understanding leaf phenology patterns and the drivers that regulate them is critical to climate change studies. In this manner, this study aimed to analyze leaf phenology patterns by near and orbital remote sensing (RS) and their relation to environmental variables. We found that the analyzed Seasonally Dry Tropical Forests site exhibited a deciduous pattern on three different observation scales that responded primarily to cumulative rainfall. The start of the growing season between near and orbital RS showed differences of seven days, which was mainly affected by the low temporal resolution and high cloud incidence in the orbital RS.

***Key words* —** remote sensing, digital cameras, caatinga, time series, start of the growing season.

1. INTRODUCTION

Phenology is the study of recurring periodic patterns of growth and development of plants and animals [1] and is strongly related to abiotic factors such as precipitation and temperature [2]. In particular, vegetation phenology is linked to important plant processes such as photosynthesis, carbon dioxide (CO_2) uptake, and transpiration [3]. Changes in these patterns have major impacts on ecosystems (e.g., food supply), and on biogeochemical cycles and processes (e.g., water, carbon, and energy cycles) that operate from local to global scales [2, 4].

Drylands – defined here as regions where potential evapotranspiration substantially exceeds precipitation – play an important role in this context, accounting for 41% of the Earth's surface and 27% of the world's forest cover [5, 6], including Seasonally Dry Tropical Forests (SDTF). Drought constraints increase leaf maintenance costs in plants, and deciduous strategy turns out to be the most common leaf exchange behavior in SDTF [7]. In summary, leaf phenology of SDTF can vary depending:1) rainfall regimes and water availability; 2) variability between species and stratification; and 3) adaptations to the environment [4, 8, 9]. These factors can promote distinguishing differences in phenological observations from different observation scales. However, little is known about the structural and functional dynamics of vegetation, as well as the physiological processes of the events that comprise the soil-root-leaf-atmosphere pathway and how these processes alter the leaf phenology.

The aim of this work is to describe the phenological patterns between three observational scales: canopy, community and landscape, based on the hypothesis that, in addition to climatic factors, the composition and diversity of plant communities can influence the seasonality of these patterns when observed by remote sensing techniques [10]. Specifically, the goals are:

a) To identify the patterns between canopy (phenological camera), community (phenological camera), and landscape (satellite); b) To correlate statistics of normalized indices and environmental variables in daily, seven-day, and monthly values; c) To detect the beginning of the growing season at the community and landscape level.

2. MATERIAL AND METHODS

The study site is located in Petrolina - Pernambuco, Brazilian Northeast, across the SDTF in Caatinga biome [8]. The climate is classified as semiarid, with mean temperature of 26.5 °C and annual precipitation of 275 mm in 2014, according to the climatological station located at the same site) (Figure 2L).

Digital images captured by a phenological camera between 9:00 a.m. and 6:00 p.m. from January to December 2014 (corresponding to 60 images per day) were used as described by [8] (Figure 1). The raw digital images (JPEG format) were first processed in the PhenoViewer software, removing invalid images. Regions of interest (ROIs) were

then extracted in the images to capture all the community (totalizing 1 ROI) as well as individual tree canopies (totalizing 9 ROIs). Note that the selection of ROIs in tree canopies took into account only visually observed leaf variations, which do not necessarily identify the species. In this manner, leaf overlap between canopies and background effects throughout the period analyzed could influence the analysis. For each ROI, the normalized indices of the green channel (Gcc), red channel (Rcc), and blue channel (Rcc) were calculated in each image. A single measurement was then extracted by taking the 90th percentile of all values observed each day, to minimize interference related to changes in lighting [8].

Figure 1 – Hemispherical image used to extract the ROI defined as a community (yellow). Individual tree canopies ROIs were also extracted from canopies in this area.

In addition, surface reflectance data from the Operational Land Imager (OLI) sensor onboard the Landsat-8 satellite (16-day temporal resolution) were used. For this data, a cloud mask from the CFMASK algorithm was used to remove pixels classified as cloud and cloud shadow in the time series between January 2014 and the first valid image in January 2015. The period of analysis was extended due to the high incidence of clouds at the end of the year and only one pixel (900 m²) was considered as a ROI. For the analysis, the Gcc was also calculated for each image and all processing was performed in Google Earth Engine [11]. A linear interpolation between null values was used to construct the time series.

Daily environmental data from the climatological station was also used [8]. These data are characterized by measurements of accumulated precipitation (mm, abbreviation: rain), average temperature (°C, abbreviation: t.air), respiration (µmol CO2 m^{-2} s^{1}), incident photosynthetically active radiation (µmol CO2 m^{-2} s^{1}, abbreviation: par), gross primary productivity (µmol CO2 m^{-2} s^{1}, abbreviation: gpp) and relative humidity (%, abbreviation: % humidity).

Pearson correlations were calculated between environmental data and normalized indices extracted from the phenological camera and Landsat-8/OLI. A Generalized Additive Mixed Model (GAMMs) was used to smooth the time series of Gcc index [8], with a degree of freedom of 30 for the phenological camera and 10 for the Landsat-8/OLI datasets. Finally, a phenological metric of the start of the growing season (SOS) was estimated using a first-order derivative model on the smoothed time series of Gcc at the community and landscape scales. All analyzes were performed in Python and R programming languages.

3. RESULTS

The Gcc index time series extracted from the phenological camera and orbital sensor enabled the identification of seasonal patterns of leaf changes (SOS, season length, and shape of the seasonal curves) at the study site and differences between canopy, community, and landscape scales (Figure 2A-K).

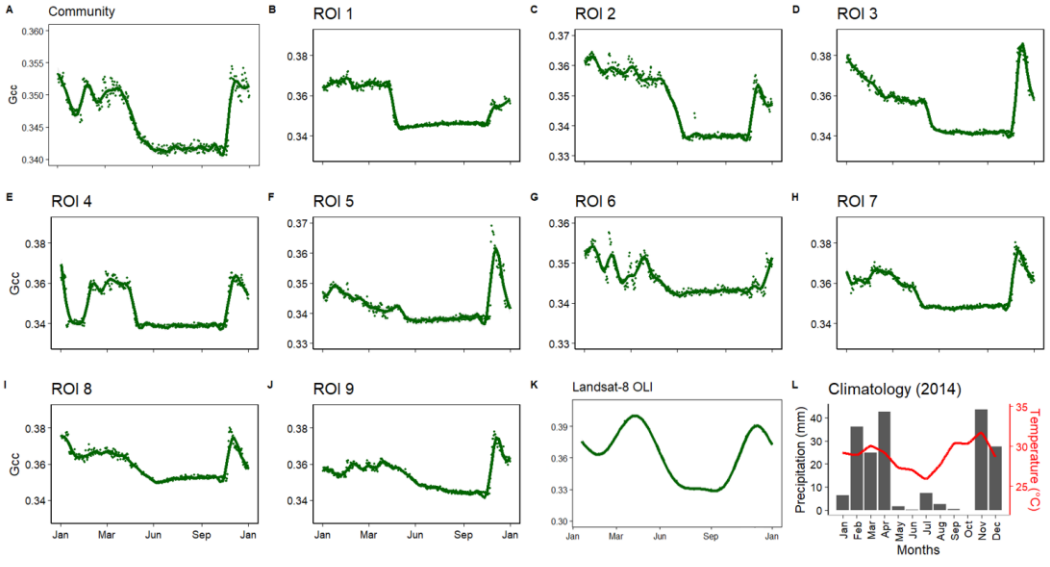

Figure 2 - Value of the daily time series Gcc adjusted by GAMMs for the ROIs obtained with the phenological camera at the community scale (A) and the canopy scale (B-J), and for the ROI obtained at the landscape scale (K). Note that the y-axis is on different scales to facilitate visualization. The green lines represent the fitted GAMM model and the green dots represent the observed data. Maximum values of precipitation (mm) and temperature (°C) monthly (L).

The Gcc curves were generally consistent with the precipitation patterns, although some small differences were observed at the canopy scale, even under the same climate regime. Despite the small number of canopy ROIs, it is observed that the variability in leaf flow associated with the composition and diversity of a community and the response between different individuals and functional types, can drive varied responses at the community and landscape scales [4, 9, 12].

Comparing the accumulated monthly average of Gcc at the community and landscape scales (Figure 3), it is observed that the patterns of start and end of the growing season are similar, with the lowest values of Gcc between June and October, coinciding with the driest months of the year. However, it is noteworthy that patterns observed by orbital remote sensing can be strongly influenced by the high incidence of invalid data (e.g., cloud and cloud shadow) and spatial and temporal resolutions. In this example, the low temporal resolution of 16-days and the lack of data between the months of February might have influenced the observed differences, as they were insufficient for detecting rapid events in leaf phenology as observed with the phenological camera.

A

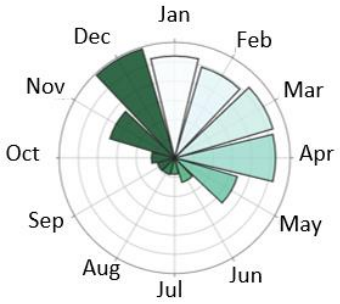

B

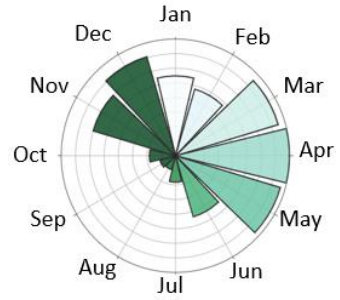

Figure 3 - Circular histogram of Gcc values by monthly average in 2014 between the phenological camera images, with radial axis scaled between 0.34 and 0.36 (A) and Landsat-8/OLI, with radial axis scaled between 0.32 and 0.40 (B).

A strong positive correlation was observed between community-scale Gcc and maximum monthly rainfall (r = 0.74, p<0.05) (Figure 4A), followed by the monthly 90th percentile (0.52, p<0.05) (Figure 4B). Considering the 90th percentile between seven days and daily data, this correlation was 0.36 (p<0.05) and 0.15 (p>0.05), respectively. Gpp was the variable with the highest positive correlations with the Gcc, with r = 0.78 (p<0.05) at the daily 90th percentile, and r = 0.93 (p<0.05) at the monthly 90th percentile. With the smoothed time series, a correlation of 0.83 (p<0.05) was obtained between community-scale Gcc and landscape-scale Gcc.

A

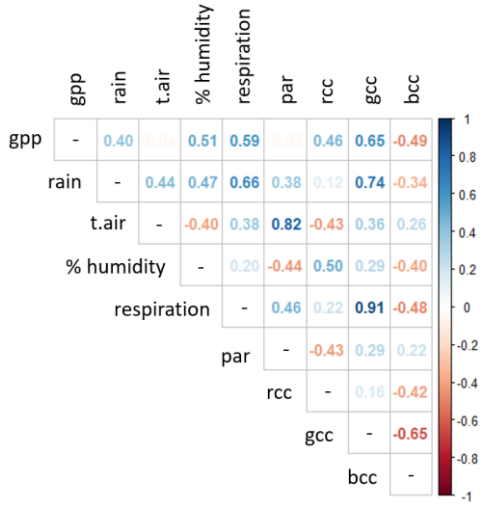

B

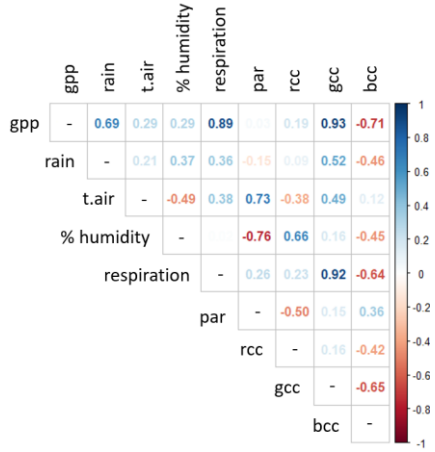

Figure 4 – Correlations observed between normalized indices (Gcc, Rcc, Bcc) at the community (90th percentile)

and environmental variables, considering the maximum-value (A) and 90th percentile (B) statistics calculated by month.

The SOS was estimated on 11/01/2014 at the community scale and on 11/08/2014 at the landscape scale (equivalent to 7 days difference), a month characterized by increased precipitation. However, no canopy-scale phenological metrics were not extracted, which may show differences.

4. DISCUSSION

The Gcc index observed at the canopy, community, and landscape scale revealed a deciduous pattern in the studied SDTF, that responded primarily to cumulative rainfall. The leaf phenology of STDF is strongly driven by water availability and the temporal and spatial variability of rainfall. As the beginning of the growing seasons in drylands is usually marked by the beginning of the rainy season, it is observed that SOS estimates are more influenced by atmospheric effects and consequently their detection is more sensitive to rapid vegetation changes. In this sense, studies using high temporal resolution orbital sensors obtained smaller differences between phenological cameras [13].

5. CONCLUSIONS

This study observed the leaf phenology of a seasonally dry tropical forest site at different scales and the relationship between environmental variables. Identifying the patterns of leaf phenology and the factors that regulated them is crucial to efficiently understanding and forecasting the impacts of climate change. However, the potential of combining orbital and near-surface remote sensing in vegetation phenology to elucidate the intrinsic factors and processes in drylands still remains poorly explored.

6. FUNDING

This research was financed by the Fundação de Amparo à Pesquisa do Estado de São Paulo (FAPESP), process nº 2022/01746-5, and in part by the Coordenação de Aperfeiçoamento de Pessoal de Nível Superior – Brasil (CAPES) - Finance Code 001**.**

REFERENCES

[1] H. Lieth. Purposes of a Phenology Book. n. 86, p. 3–19, 1974.

[2] S. Piao, Q. Liu, A. Chen, I. A. Janssens, Y. Fu, J. Dai, L. Liu, X. Lian, M. Shen, X. Zhu. Plant phenology and global climate change: Current progresses and challenges. *Global Change Biology*, v. 25, n. 6, p. 1922–1940, 2019.

[3] D. Helman. Land surface phenology: What do we really 'see' from space? *Science of the Total Environment*, v. 618, p. 665–673, 2018.

[4] W. K. Smith, M. P. Dannenberg, D. Yan, S. Herrmann, M. L. Barnes, G. A. Barron-Gafford, J. A. Biederman, S. Ferrenberg, A. M. Fox, A. Hudson, J. F. Knowles, N. Macbean, D. J. P. Moore, P. L. Nagler, S. C. Reed, W. A. Rutherford, R. L. Scott, X. Wang, J, Yang. Remote sensing of dryland ecosystem structure and function: Progress, challenges, and opportunities. *Remote Sensing of Environment*, v. 233, n. August, p. 111401, 2019.

[5] FAO. Trees, forests and land use in drylands: the first global assessment-Full report. FAO Forestry Paper No. 184. Rome. [s.l: s.n.]. 31 p., 2019.

[6] UNCC. Part Two, Chapter 2. In: DESERTIFICATION, U. N. C. TO C. (Ed.). Global Land Outlook first edition. [s.l: s.n.]. p. 381–658, 2017.

[7] P. L. Morellato, N. Neves, B. Alberton, M. Moura, R. Lima, E. Souza, R. Souza, J. Raliuson Silva, R. Miatto, T. Domingues, and Cunha, J., 2022, May. Phenocams as a tool to investigate leaf economic spectrum relations in Seasonally Dry Tropical Forests. In *EGU General Assembly Conference Abstracts* (pp. EGU22-13004).

[8] B. Alberton, R. Da Silva Torres, T. S. F. Silva, H. R. D. Rocha, M. Moura and L. P. Morellato. Leafing Patterns and Drivers across Seasonally Dry Tropical Communities. *Remote Sensing*, 11(19), 2267, 2019.

[9] R. Whitley, J. Beringer, L. B. Hutley, G. Abramowitz, M. G. De Kauwe, B. Evans, V. Haverd, L. Li, C. Moore, Y. Ryu, S. Scheiter, S. J. Schymanski, B. Smith, Y. P. Wang, M. Williams, Q. Yu. Challenges and opportunities in land surface modelling of savanna ecosystems. *Biogeosciences*, v. 14, n. 20, p. 4711–4732, 2017.

[10] Dronova & S. Taddeo. Remote sensing of phenology: Towards the comprehensive indicators of plant community dynamics from species to regional scales. *Journal of Ecology*, 2022.

[11] N. Gorelick, M. Hancher, M. Dixon, S. Ilyushchenko, D. Thau, And R. Moore, Google Earth Engine: Planetary-scale geospatial analysis for everyone. *Remote sensing of Environment*, 202, pp.18-27, 2017.

[12] C. E. Moore, T. Brown, T. F. Keenan, R. A. Duursma, Van A. I. J. M. Dijk, Beringer, D. Culvenor, B. Evans, A. Huete, L. B. Hutley, S. Maier, N. Restrepo-Coupe, O. Sonnentag, A. Specht, J. R. Taylor, E. Van Gorsel, M. J. Liddell. Reviews and syntheses: Australian vegetation phenology: New insights from satellite remote sensing and digital repeat photography. *Biogeosciences*, v. 13, n. 17, p. 5085–5102, 2016.

[13] L. Cui, J. Shi. Evaluation and comparison of growing season metrics in arid and semi-arid areas of northern China under climate change. *Ecological Indicators*, v. 121, n. August 2020, p. 107055, 2021.